ARTICLE

Improvement of the Light-Harvesting Efficiency in Polymer/Fullerene Bulk Heterojunction Solar Cells by Interfacial Dye Modification

Satoshi Honda, Takahiro Nogami, Hideo Ohkita,* Hiroaki Benten, and Shinzaburo Ito

Department of Polymer Chemistry, Graduate School of Engineering, Kyoto University, Katsura, Nishikyo, Kyoto 615-8510, Japan

ABSTRACT Enhancement of the light-harvesting efficiency in poly(3-hexylthiophene)/fullerene derivative (P3HT/PCBM) bulk heterojunction solar cells has been demonstrated by the introduction of near-infrared phthalocyanine molecules as the third component at the P3HT/PCBM interface. The introduction of silicon phthalocyanine derivative (SiPc) increased the short-circuit current density and hence improved the overall power conversion efficiency by 20%, compared to the P3HT/PCBM control device. For P3HT/PCBM/SiPc devices, two distinct external quantum efficiency (EQE) peaks were observed at wavelengths for the absorption bands of SiPc as well as P3HT before and after thermal annealing, suggesting that SiPc molecules are located at the P3HT/PCBM interface because of crystallization of the P3HT and PCBM domains. Furthermore, the EQE for the device increased even at wavelengths for the absorption band of P3HT by the introduction of SiPc molecules. This indicates that P3HT excitons can be dissociated into charge carriers more efficiently in the presence of SiPc molecules at the P3HT/PCBM interface by energy transfer from P3HT to SiPc molecules. These findings suggest that there are two origins for the increase in the photocurrent by the introduction of SiPc; SiPc molecules serve not only as a light-harvesting photosensitizer but also as an energy funnel for P3HT excitons at the P3HT/PCBM interface.

KEYWORDS: polymer/fullerene solar cell • donor/acceptor interface • near-infrared dye • dye modification • light harvesting

INTRODUCTION

Polymer/fullerene bulk heterojunction (BHJ) solar cells have attracted much attention because they are considered to be a promising candidate for a lightweight, flexible, cost-effective, large-area, and renewable energy source (1−9). Since the 1990s, power conversion efficiencies (PCEs) of polymer/fullerene solar cells have been steadily improved, and in recent years, operational stabilities of such devices have also been studied for practical application (10−15). Currently, the most effective materials employed in polymer/fullerene BHJ solar cells are regioregular poly(3-hexylthiophene) (P3HT; Figure 1a) as the donor and 1-(3-methoxycarbonyl)propyl-1-phenyl[6,6]methanofullerene (PCBM; Figure 1b) as the acceptor. Recently, PCEs approaching 5% have been reported by several groups for this donor/acceptor combination (16−19). Furthermore, short-circuit external quantum efficiencies (EQEs) exceed 70% for such devices (18, 19), suggesting that most excitons can contribute to the photocurrent generation although photoluminescence (PL) from P3HT is still observed after thermal annealing (18). In other words, it can safely be said that there is little room for significant improvement in the short-circuit current density (J_{SC}) for BHJ solar cells based on only P3HT and PCBM.

To collect the solar light more efficiently, a variety of low-band-gap polymers have been developed over the last several years (20−23) because P3HT can absorb only ~25% of the total number of photons in the solar light (9). It is striking that a PCE of over 5% has been reported for blend films of a low-band-gap polymer and the C_{70} derivative of PCBM (23, 24). At this moment, however, there are few successful reports on low-band-gap polymer-based solar cells, partly because it is difficult to synthesize low-band-gap polymers with a high charge mobility (25). On the other hand, dye sensitization is another approach to improving the light-harvesting efficiency, but there have been few successful reports for improving the light-harvesting efficiency in polymer BHJ solar cells. Only recently, the dye-sensitization effect has been demonstrated for polymer/fullerene BHJ solar cells (26). In general, dye molecules are simply blended as the third component to absorb the solar light at longer wavelengths that the original donor and acceptor materials cannot harvest. This is a simple and versatile method, and therefore various dye molecules are available. In most cases, however, dye introduction rarely improved but rather degraded the device performance. This is considered to be due to the formation of dye aggregations in blend films, which would reduce the absorption efficiency or the charge mobility of the active layer (27−29).

Herein we report the photovoltaic properties of BHJ solar cells based on P3HT/PCBM blends incorporated with a dye molecule. To examine the relationship between the device performance and the formation of dye aggregations in the

* Corresponding author. E-mail: ohkita@photo.polym.kyoto-u.ac.jp.
Received for review December 11, 2008 and accepted February 17, 2009

DOI: 10.1021/am800229p

© 2009 American Chemical Society

Published on Web 03/16/2009

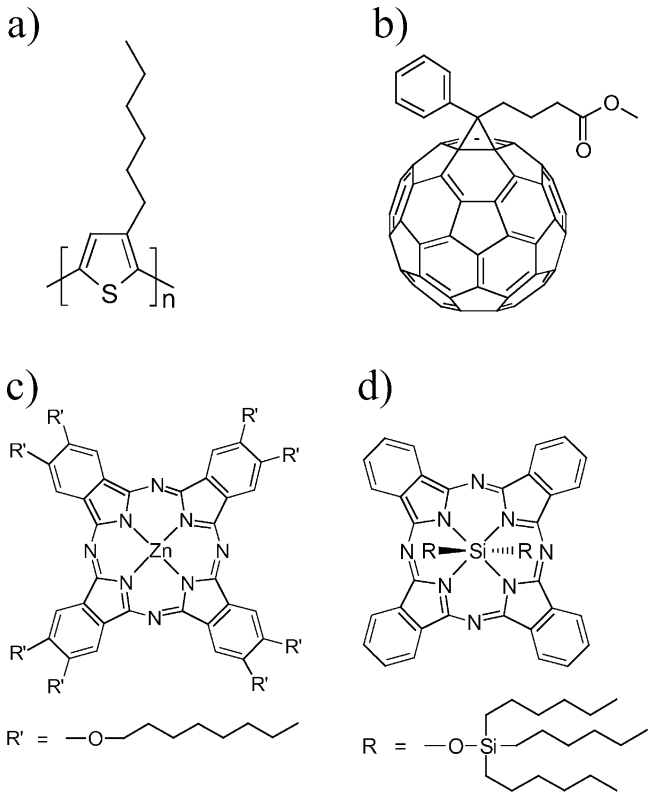

FIGURE 1. Chemical structures of (a) the donor material P3HT, (b) the acceptor material PCBM, and the near-infrared dyes (c) ZnPc and (d) SiPc. The ZnPc molecule is a planar structure, while the SiPc molecule is a bulky structure with bis(trihexylsilyl oxide) groups in the axial direction perpendicular to the phthalocyanine plane.

blend film, we employ two near-infrared dye molecules with different structures: one is zinc 2,3,9,10,16,17,23,24-octakis(octyloxy)-29*H*,31*H*-phthalocyanine (ZnPc; Figure 1c), and the other is silicon phthalocyanine bis(trihexylsilyl oxide) (SiPc; Figure 1d). For a P3HT/PCBM/SiPc ternary blend device, J_{SC} increased from 6.5 to 7.9 mA cm^{-2} and, hence, the overall PCE improved from 2.2 to 2.7% by introduction of the dye molecule. This improvement suggests that the appropriate allocation of dye molecules at the donor/acceptor interface without the formation of dye aggregations is crucial for the effective dye sensitization in polymer/fullerene solar cells.

EXPERIMENTAL METHODS

All devices were fabricated as follows: indium/tin oxide (ITO)-coated glass substrates (10 Ω per square) were washed by ultrasonication in toluene, acetone, and ethanol for 15 min, dried with N_2, and then cleaned with a UV O_3 cleaner (Nippon Laser & Electronics NL-UV253S) for 30 min. A thin layer (ca. 40 nm) of poly(3,4-ethylenedioxythiophene) oxidized with poly(4-styrenesulfonate) (PEDOT:PSS; H. C. Starck PH500) was spin-coated onto the cleaned substrates at a spin rate of 3000 rpm, and the layer was dried at 140 °C for 10 min in air. A blend layer of P3HT/PCBM/dye (100 nm) was spin-coated from a chlorobenzene solution on the PEDOT:PSS film at 1200 rpm for 60 s. The blend solution was prepared as follows: P3HT (Plextronics, regioregularity > 98%, number-average molecular weight, $M_n \sim 45\,000-65\,000$ g mol^{-1}) was dissolved in chlorobenzene (10 mg mL^{-1}), and the solution was stirred at 40 °C overnight. To the solution were added PCBM (Frontier Carbon; 10 mg mL^{-1}) and dye (Aldrich, ZnPc or SiPc; 0.7 mg mL^{-1}). Note

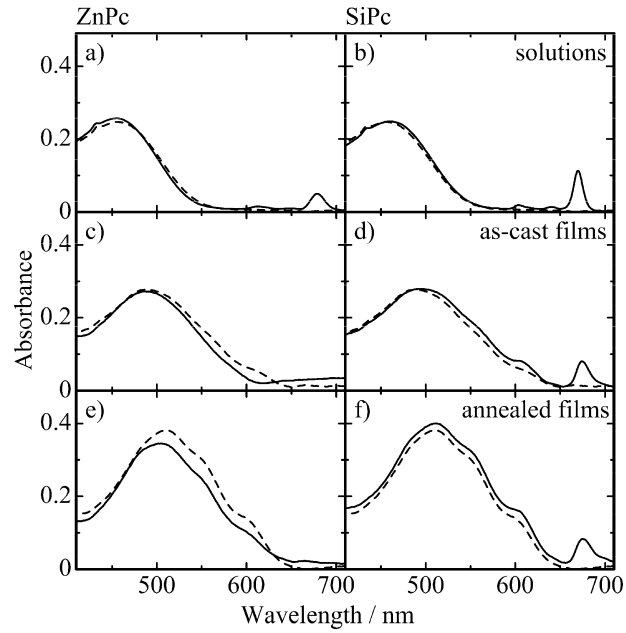

FIGURE 2. Absorption spectra of blend solutions, as-cast films, and annealed films with (solid lines) and without dye molecules (broken lines): (a) P3HT/PCBM/ZnPc solutions, (b) P3HT/PCBM/SiPc solutions, (c) P3HT/PCBM/ZnPc as-cast films, (d) P3HT/PCBM/SiPc as-cast films, (e) P3HT/PCBM/ZnPc annealed films, and (f) P3HT/PCBM/SiPc annealed films.

that the dye concentration was optimized in the range from 0.1 to 2.0 mg mL^{-1}. The blend solution was filtered with a 0.45-μm poly(tetrafluoroethylene) filter before the spin coating. The active layer was thermally annealed at 150 °C for 30 min in a N_2-filled glovebox. A thin layer of TiO_x (<10 nm) was prepared by the spin coating from a dehydrated ethanol solution of titanium isopropoxide (Aldrich) at 2000 rpm for 60 s (30). Finally, the aluminum electrode (70 nm) was thermally deposited on top of the TiO_x layer at 2.5×10^{-4} Pa. For comparison, P3HT/PCBM control devices without dye were also prepared separately under the same conditions to give the same active layer thickness.

Absorption and PL spectra were measured with a spectrophotometer (Hitachi model U-3500) and a spectrofluorometer (Jasco model FP-6600), respectively. The film thickness was evaluated with an atomic force microscope (Shimadzu model SPM-9500J) in the contact mode at room temperature. The $J-V$ characteristics were measured with a direct-current voltage and a current source/monitor (Advantest model R6243) in the dark and under illumination with AM1.5G simulated solar light with 100 mW cm^{-2}. The light intensity was corrected with a calibrated silicon photodiode reference cell (Peccell model PEC-SI01). The photocurrent action spectra were measured with a digital electrometer (Advantest model R8252) under monochromatic light illumination from a 500-W xenon lamp (Thermo Oriel model 66921) with optical cut filters and a monochromator (Thermo Oriel, UV−visible Conerstone). The active area of the device was 0.07 cm^{-2}. The illumination was carried out from the ITO side in air. At least 10 devices were fabricated to ensure reproducibility of the $J-V$ characteristics.

RESULTS

1. Absorption Spectra. We first compare the absorption spectra of the two dye molecules in solutions and in blend films before and after annealing. In blend solutions, as shown in parts a and b of Figure 2, a large and broad absorption and a small and sharp absorption were observed

at around 460 and 670 nm, which are ascribable to P3HT and dye (ZnPc or SiPc), respectively. The absorption spectrum of each blend solution is a simple superposition of the P3HT and dye spectra because of little contribution of PCBM in the same wavelength range, indicating homogeneous mixing and no interaction in the ground state. On the other hand, the blend films showed different absorption spectra between ZnPc and SiPc. As shown in parts c and d of Figure 2, the P3HT/PCBM/ZnPc blend film exhibits a distinct absorption band of P3HT at around 500 nm and a significantly broadened and decreased absorption band of ZnPc at around 670 nm, while the P3HT/PCBM/SiPc blend film exhibits distinct absorption bands of P3HT and SiPc at around 500 and 670 nm, respectively, as with the blend solution. Note that ZnPc molecules certainly exist in the blend film because the ZnPc absorption was observed for a solution prepared by dissolving the blend film again. Therefore, the decrease in the absorption of ZnPc indicates the formation of dye aggregations in the film, which would reduce the effective absorption coefficient (31, 32). As shown in parts e and f of Figure 2, a similar tendency was observed for the blend films after annealing: the ZnPc absorption was still negligible, but the SiPc absorption remained the same as that before annealing. It is noteworthy that the P3HT/PCBM/SiPc blend film exhibits a large absorption of P3HT with a distinct shoulder at around 600 nm comparable to those for the control device without SiPc, which are indicative of crystallization of P3HT (33, 34), while the P3HT/PCBM/ZnPc blend film exhibits relatively smaller changes in the absorption of P3HT. This difference suggests that ZnPc molecules disturb the crystallization of P3HT, while SiPc molecules do not at all. These spectral differences are discussed later in terms of molecular structures.

2. $J-V$ Characteristics. We turn now to the device performance of these two blend films with different dye molecules. Figure 3a shows the $J-V$ characteristics of P3HT/PCBM/ZnPc solar cells and P3HT/PCBM control cells before and after annealing under AM1.5G illumination from a calibrated solar simulator with an intensity of 100 mA cm^{-2}. The averaged device parameters of these cells are summarized in Table 1. Before the thermal annealing, the $J-V$ curve (thin solid line) was almost the same as that for the control cell without ZnPc (thin broken line). After the thermal annealing, J_{SC} significantly increased and was comparable to that for the control cell without ZnPc (thick broken lines), while the fill factor (FF) was much smaller than that for the control cell. As a result, the introduction of ZnPc decreased PCE from 2.2 to 1.1%. Such a poorer performance can be ascribed to the formation of dye aggregations in blend films. In particular, the $J-V$ curve with an inflection point has been occasionally seen for organic solar cells, indicating that there is a transport-limiting interface close to the aluminum electrode (35, 36). Therefore, aggregations of ZnPc molecules are also likely to limit the transport of photogenerated charges at the interface. On the other hand, as shown in Figure 3b and Table 1, the P3HT/PCBM/SiPc device exhibits a distinguished increase in J_{SC} to 7.9 mA cm^{-2} after the thermal annealing, which is even higher than that for the control device (6.5 mA cm^{-2}). It should be noted that FF remained the same as that for the control device without SiPc even after the thermal annealing, which would induce the formation of dye aggregations. As a result, the overall performance improved to PCE = 2.7%. This finding suggests that the appropriate selection of dye molecules is crucial for improving the device performance effectively.

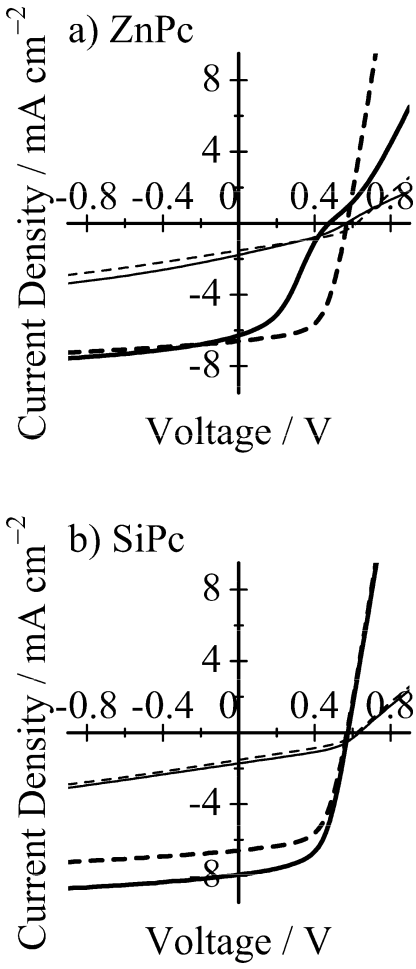

FIGURE 3. $J-V$ characteristics of P3HT/PCBM blend films with (solid lines) and without dye (broken lines) before (thin lines) and after annealing (thick lines): (a) P3HT/PCBM/ZnPc; (b) P3HT/PCBM/SiPc.

Table 1. Averaged Device Parameters of P3HT/PCBM Solar Cells with and without Dye[a]

	J_{SC}/mA cm^{-2}	V_{OC}/V	FF	PCE/%
P3HT/PCBM	1.5	0.60	0.33	0.30
P3HT/PCBM/ZnPc	1.9	0.58	0.32	0.35
P3HT/PCBM/SiPc	2.1	0.64	0.43	0.58
P3HT/PCBM (annealed)	6.5	0.58	0.59	2.2
P3HT/PCBM/ZnPc (annealed)	6.2	0.48	0.37	1.1
P3HT/PCBM/SiPc (annealed)	7.9	0.58	0.59	2.7

[a] All of the parameters are averaged values for at least 10 devices.

3. EQE Spectra. In order to address the origin of the increase in J_{SC} by the addition of SiPc, we measured the EQE spectra of P3HT/PCBM/SiPc and P3HT/PCBM/ZnPc devices for comparison. In the EQE spectra of the P3HT/PCBM/ZnPc devices, as shown in Figure 4a, the photocurrent peak was

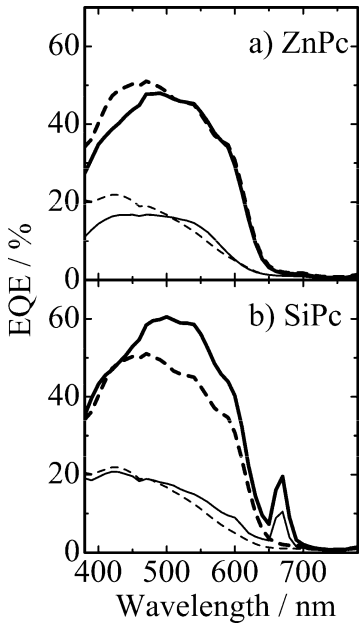

FIGURE 4. EQE spectra of P3HT/PCBM blend films with (solid lines) and without dye (broken lines) before (thin lines) and after annealing (thick lines): (a) P3HT/PCBM/ZnPc; (b) P3HT/PCBM/SiPc.

observed only in the wavelength range (400−600 nm) of the P3HT absorption and no photocurrent signal was observed in the wavelength range (650−700 nm) of the ZnPc absorption, which is in agreement with the absorption spectra mentioned before. On the other hand, as shown in Figure 4b, the P3HT/PCBM/SiPc devices exhibit two EQE peaks in the wavelength range of the P3HT absorption and also in the longer wavelength range (650−700 nm) of the SiPc absorption. Before the thermal annealing, the EQE corresponding to the P3HT absorption (470−600 nm) was comparable to that for the control device without SiPc (∼20%). The EQE corresponding to the SiPc absorption (650−700 nm) was as high as 10%, which is clear evidence that direct photoexcitation of SiPc does contribute to photocurrent generation. After the thermal annealing, the EQE corresponding to direct photoexcitation of SiPc (650−700 nm) increased up to 20% compared to that before annealing (∼10%), suggesting that the thermal annealing results in an increase in the number of SiPc molecules that can directly contribute to the photocurrent. More interestingly, the EQE corresponding to the P3HT absorption (470−600 nm) also increased to ∼60% compared to that for the control device without SiPc (∼50%), suggesting that SiPc molecules are not directly involved in the photoabsorption but, nonetheless, promote charge generation from P3HT excitons indirectly. In other words, there are two origins for the increase in J_{SC} by the addition of SiPc molecules: one is that the direct contribution of SiPc to the photocurrent results from photoexcitation of the incorporated SiPc itself, and the other is that the indirect contribution of SiPc to the photocurrent results from the improvement in the charge generation from P3HT excitons in the presence of SiPc. From the EQE spectra, the contribution of each mechanism to the increase in J_{SC} was evaluated to be 0.4 mA cm^{-2} for the direct mechanism and 1.0 mA cm^{-2} for the indirect mechanism.

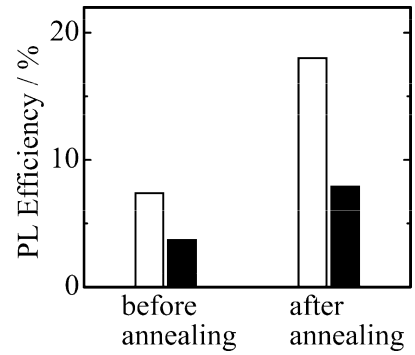

FIGURE 5. PL efficiency of P3HT/PCBM/SiPc (closed bars) and P3HT/PCBM (open bars) blend films before and after annealing. The efficiency was evaluated as the ratio of the PL intensity of blend films to that of a P3HT pristine film when P3HT was selectively excited at 550 nm. The PL intensity observed at 700 nm was corrected by variation of the absorption at the excitation wavelength.

Therefore, the increase in J_{SC} is mainly due to the indirect contribution of SiPc to the improvement in the charge generation from P3HT excitons rather than the direct photoabsorption of SiPc molecules. We will discuss each mechanism later in detail.

4. PL Quenching. We furthermore measured the PL efficiency of P3HT in blend films with acceptor materials (PCBM or SiPc) to obtain an in-depth understanding of the quenching mechanism of P3HT excitons in the ternary blends. The PL efficiency was evaluated as the ratio of the PL intensity at 700 nm of the blend films to that of the pristine P3HT film when P3HT was selectively excited at 550 nm. Before the thermal annealing, as shown in Figure 5, the PL efficiency was lower than 8% for both P3HT/PCBM and P3HT/PCBM/SiPc blend films. The low PL efficiency suggests that most of the P3HT excitons can arrive at the interface because of the homogeneous mixture of P3HT and PCBM in blend films. After the thermal annealing, the PL efficiency of the P3HT/PCBM blend increased to 18%, which is consistent with previous reports (18, 37). The increase in the PL efficiency suggests that fewer P3HT excitons can arrive at the interface after the thermal annealing, which is ascribable to enlargement of the P3HT domain because of crystallization. On the other hand, the PL efficiency of the P3HT/PCBM/SiPc film was as low as 8% even after annealing, which is comparable to that of the P3HT/PCBM film before annealing. As mentioned before, the introduction of SiPc molecules does not disturb the crystallization of P3HT. Therefore, these results suggest that there is an efficient exciton-harvesting mechanism in the P3HT/PCBM/SiPc ternary blend films.

DISCUSSION

We start off our discussion by considering the difference in the absorption spectra and the device performance between the two dye molecules (ZnPc and SiPc) with different structures. The ZnPc dye can be regarded as a planar molecule and is therefore likely to stack in the direction normal to the phthalocyanine plane, resulting in the formation of dye aggregations. On the other hand, the SiPc dye has two bulky groups in the axial direction perpendicular to

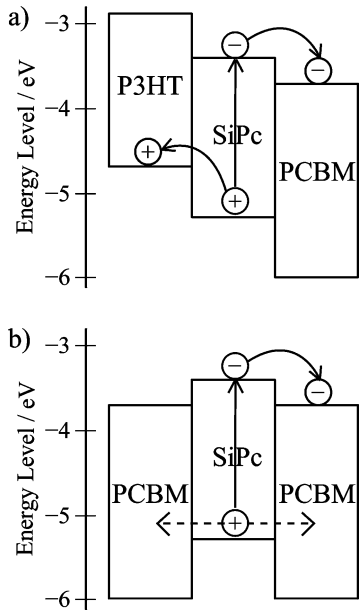

FIGURE 6. Energy diagrams of SiPc molecules and the surrounding materials: (a) SiPc located at the interface between P3HT and PCBM; (b) SiPc located in the PCBM domain.

the phthalocyanine plane, which probably inhibit effective stacking of the π-conjugation plane and hence suppress the formation of dye aggregations. As mentioned before, the difference in the absorption spectra and the device performance can be explained in terms of the formation of dye aggregations in blend films. In previous reports on BHJ solar cells incorporated with dye molecules, planar dye molecules such as ZnPc have been generally employed and hence the formation of dye aggregations has been the main obstacle to improving the device performance (28, 29). We therefore conclude that the selection of bulky dyes such as SiPc is key to the development of ternary BHJ solar cells without the formation of dye aggregations.

Next, we discuss the location of SiPc dye molecules in blend films. As shown in Figure 6a, SiPc excitons located at the interface of P3HT/PCBM can inject an electron into PCBM and a hole into P3HT, because there are energetic cascades in both the lowest unoccupied molecular orbital (LUMO) and highest occupied molecular orbital (HOMO) levels (38−41). This energetic cascade is essential for dye sensitization at the interface. On the other hand, SiPc excitons located in a PCBM domain, as shown in Figure 6b, can inject an electron into the PCBM domain but cannot inject a hole into the surrounding PCBM domain because of the lower HOMO level of PCBM. Much the same is true for SiPc excitons located in a P3HT domain. In other words, only SiPc molecules located at the interface of P3HT/PCBM can contribute to the photocurrent generation. Therefore, our observation of the photocurrent originating from the SiPc absorption indicates that some SiPc molecules are located at the P3HT/PCBM interface even before the thermal annealing. Furthermore, it can be said that more SiPc molecules contribute to the photocurrent after the thermal annealing, because as mentioned before the EQE at 670 nm increased from 10 to 20% while the absorbance remained the same. This is probably because the charge collection efficiency is improved by the formation of interpenetrating networks of P3HT and PCBM by the thermal annealing. In addition, it is possible that the number of SiPc molecules located at the P3HT/PCBM interface, which can contribute to the photocurrent generation, is simply increased by the thermal annealing. The EQE after the thermal annealing (~20%) is comparable to the absorption at the same wavelength 670 nm, suggesting that the majority of SiPc molecules incorporated are localized at the interface. We speculate that the localization of SiPc molecules at the interface is due to crystallization of P3HT and aggregation of nanocrystalline PCBM domains upon annealing as reported previously (33, 42). In other words, SiPc molecules located in P3HT or PCBM domains could be expelled from each domain into the interface by crystallization of P3HT and aggregation of nanocrystalline PCBM domains. We therefore emphasize that the selection of crystalline materials such as P3HT and PCBM as a matrix is crucial for the localization of dye molecules at the interface where the charge separation can occur efficiently, which is also key to the development of interfacial dye modification in ternary BHJ solar cells.

Finally, we discuss the mechanism of dye sensitization in P3HT/PCBM/SiPc ternary blends. As mentioned before, there are two mechanisms for the increase in J_{SC} by the addition of SiPc molecules. One is that the additional absorption of SiPc molecules contributes to the increase in J_{SC} directly. In the present study, this direct contribution is not so large because of the narrow absorption band of SiPc molecules, which can harvest the solar light only at a limited spectral window. Dye molecules with a wider absorption band would provide a larger photocurrent. The other mechanism is that SiPc molecules promote the charge separation from P3HT excitons at the interface, although they do not absorb photons directly. Previously, we reported a similar result for a P3HT/TiO_2 bilayered hybrid solar cell with chemical modification of the TiO_2 surface with a ruthenium complex dye (43). In the hybrid cell, the EQE originating from P3HT increased by the introduction of dye molecules at the interface, which can be explained in terms of Förster energy transfer from P3HT to the ruthenium complex. Such efficient light harvesting by using energy transfer has also been reported for another hybrid solar cell (44, 45). The same is true for the present system. Simple calculation assuming point dipoles gives a large Förster radius of beyond 3 nm for energy transfer from P3HT to SiPc. The energy transfer rate from P3HT to SiPc is estimated to be as fast as $\sim 8 \times 10^{12}$ s^{-1} for a spatial separation of 1 nm, which is over a 100 times faster than the energy migration rate among P3HT at the same spatial separation. As shown in Figure 7c, therefore, the efficient long-range Förster energy transfer can collect P3HT excitons that could not reach the interface only by repetition of short-range excitation energy hoppings (Figure 7b). Furthermore, the Förster energy transfer is not random diffusion but directional transport from a donor to an acceptor molecule and thereby can harvest P3HT donor excitons more efficiently into the SiPc acceptor at the

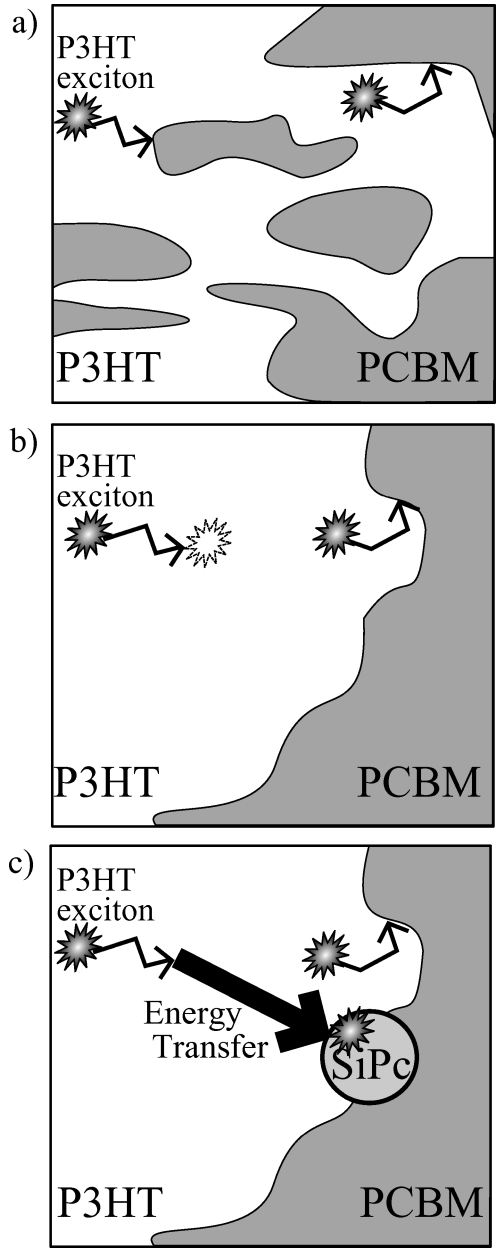

FIGURE 7. Schematic illustrations of the donor/acceptor interface: (a) before annealing, each domain is so small that most excitons can reach the interface; (b) after annealing, some excitons cannot reach the interface because of the larger domain size; (c) after annealing and in the presence of SiPc, even excitons generated far away can reach the interface by energy transfer to the SiPc molecule.

interface. In other words, the efficient long-range Förster energy transfer can increase the effective exciton diffusion length, which can explain the lower PL efficiency of the P3HT/PCBM/SiPc ternary blend film (Figure 5). The highly efficient Förster energy transfer from P3HT to SiPc supports our estimation that the majority of SiPc molecules are located at the interface because SiPc molecules in P3HT domains would quench P3HT excitons efficiently and cause a decrease in J_{SC}, but this is not the case. Note that the advantage of the Förster energy transfer would be undistinguished if P3HT and PCBM were well mixed so that most excitons could arrive at the interface even without dye molecules, as shown in Figure 7a. This situation can apply to the ternary blend before annealing because the EQE originating from P3HT and the PL efficiency were comparable to those for P3HT/PCBM blends without dye (Figures 4 and 5). From these results, we conclude that the exciton harvesting in polymer BHJ solar cells can be efficiently improved by the long-range energy transfer of incorporated dye molecules with a large spectral overlap with donor materials.

CONCLUSIONS

In summary, we have shown dye-sensitized polymer/fullerene BHJ solar cells with the improved photocurrent and PCE compared to control BHJ cells without the dye. The key to the improvement is the allocation of dye molecules at the donor/acceptor interface without the formation of dye aggregations. Such dye molecules located at the interface can contribute to the photocurrent generation by direct photoexcitation and also harvest excitons more efficiently through long-range energy transfer to the dye molecule. We demonstrated that the key requirement can be achieved by following two appropriate selections of device materials. One is the selection of dyes with bulky groups such as SiPc to suppress the formation of dye aggregations, which would reduce the effective absorption coefficient. Of course, it is essential for dye sensitization that there are energetic cascades at the interface in both the LUMO and HOMO levels. A large spectral overlap between the dye absorption and the donor fluorescence is also beneficial for efficient long-range energy transfer. The other is the selection of matrix materials likely to be crystallized such as P3HT and PCBM, which results in the localization of dye molecules at the interface where the charge separation can occur efficiently. The selection of these materials is important for the design of dye-sensitized BHJ solar cells.

Acknowledgment. This work was partly supported by the Global COE program (International Center for Integrated Research and Advanced Education in Materials Science) and by the Integrative Industry—Academia Partnership (IIAP) project including Kyoto University, Hitachi, Ltd., and Mitsubishi Chemical Corp.

REFERENCES AND NOTES

(1) Hoppe, H.; Sariciftci, N. S. *J. Mater. Chem.* **2006**, *16*, 45–61.
(2) Günes, S.; Neugebauer, H.; Sariciftci, N. S. *Chem. Rev.* **2007**, *107*, 1324–1338.
(3) Brabec, C. J.; Durrant, J. R. *MRS Bull.* **2008**, *33*, 670–675.
(4) Thompson, B. C.; Fréchet, J. M. J. *Angew. Chem., Int. Ed.* **2008**, *47*, 58–77.
(5) Krebs, F. C.; Alstrup, J.; Spanggard, H.; Larsenb, K.; Kold, E. *Sol. Energy Mater. Sol. Cells* **2004**, *83*, 293–300.
(6) Dennler, G.; Lungenschmied, C.; Neugebauer, H.; Sariciftci, N. S.; Labouret, A. *J. Mater. Res.* **2005**, *20*, 3224–3233.
(7) Lungenschmied, C.; Dennler, G.; Neugebauer, H.; Sariciftci, N. S.; Glatthaar, M.; Meyer, T.; Meyer, A. *Sol. Energy Mater. Sol. Cells* **2007**, *91*, 379–384.
(8) Krebs, F. C.; Spanggard, H.; Kjær, T.; Biancardo, M.; Alstrup, J. *Mater. Sci. Eng. B* **2007**, *138*, 106–111.
(9) Smestad, G. P.; Krebs, F. C.; Lampert, C. M.; Granqvist, C. G.; Chopra, K. L.; Mathew, X.; Takakura, H. *Sol. Energy Mater. Sol. Cells* **2008**, *92*, 371–373.
(10) Krebs, F. C.; Spanggard, H. *Chem. Mater.* **2005**, *17*, 5235–5237.

(11) Katz, E. A.; Gevorgyan, S.; Orynbayev, M. S.; Krebs, F. C. *Eur. Phys. J. Appl. Phys.* **2007**, *36*, 307–311.
(12) Jørgensen, M.; Norrman, K.; Krebs, F. C. *Sol. Energy Mater. Sol. Cells* **2008**, *92*, 686–714.
(13) Hauch, J. A.; Schilinsky, P.; Choulis, S. A.; Childers, R.; Biele, M.; Brabec, C. J. *Sol. Energy Mater. Sol. Cells* **2008**, *92*, 727–731.
(14) Krebs, F. C. *Sol. Energy Mater. Sol. Cells* **2008**, *92*, 715–726.
(15) Gevorgyan, S. A.; Krebs, F. C. *Chem. Mater.* **2008**, *20*, 4386–4390.
(16) Ma, W.; Yang, C.; Gong, X.; Lee, K.; Heeger, A. J. *Adv. Funct. Mater.* **2005**, *15*, 1617–1622.
(17) Li, G.; Shrotriya, V.; Huang, J.; Yao, Y.; Moriarty, T.; Emery, K.; Yang, Y. *Nat. Mater.* **2005**, *4*, 864–868.
(18) Kim, Y.; Cook, S.; Tuladhar, S. M.; Choulis, S. A.; Nelson, J.; Durrant, J. R.; Bradley, D. D. C.; Giles, M.; McCulloch, I.; Ha, C.-S.; Ree, M. *Nat. Mater.* **2006**, *5*, 197–203.
(19) Kim, J. Y.; Kim, S. H.; Lee, H.-H.; Lee, K.; Ma, W.; Gong, X.; Heeger, A. J. *Adv. Mater.* **2006**, *18*, 572–576.
(20) Bundgaard, E.; Krebs, F. C. *Sol. Energy Mater. Sol. Cells* **2007**, *91*, 954–985.
(21) Shaheen, S. E.; Vangeneugden, D.; Kiebooms, R.; Vanderzande, D.; Fromherz, T.; Padinger, F.; Brabec, C. J.; Sariciftci, N. S. *Synth. Met.* **2001**, *121*, 1583–1584.
(22) Yao, Y.; Shi, C.; Li, G.; Shrotriya, V.; Pei, Q.; Yang, Y. *Appl. Phys. Lett.* **2006**, *89*, 153507.
(23) Peet, J.; Kim, J. Y.; Coates, N. E.; Ma, W. L.; Moses, D.; Heeger, A. J.; Bazan, G. C. *Nat. Mater.* **2007**, *6*, 497–500.
(24) Lee, J. K.; Ma, W. L.; Brabec, C. J.; Yuen, J.; Moon, J. S.; Kim, J. Y.; Lee, K.; Bazan, G. C.; Heeger, A. J. *J. Am. Chem. Soc.* **2008**, *130*, 3619–3623.
(25) Mühlbacher, D.; Scharber, M.; Morana, M.; Zhu, Z.; Waller, D.; Gaudiana, R.; Brabec, C. *Adv. Mater.* **2006**, *18*, 2884–2889.
(26) Peet, J.; Tamayo, A. B.; Dang, X.-D.; Seo, J. H.; Nguyen, T.-Q. *Appl. Phys. Lett.* **2008**, *93*, 163306.
(27) Ltaief, A.; Chaâbane, R. B.; Bouazizi, A.; Davenas, J. *Mater. Sci. Eng. C* **2006**, *26*, 344–347.
(28) Dastoor, P. C.; McNeill, C. R.; Frohne, H.; Foster, C. J.; Dean, B.; Fell, C. J.; Belcher, W. J.; Campbell, W. M.; Officer, D. L.; Blake, I. M.; Thordarson, P.; Crossley, M. J.; Hush, N. S.; Reimers, J. R. *J. Phys. Chem. C* **2007**, *111*, 15415–15426.
(29) Kaulach, I.; Muzikante, I.; Gerca, L.; Plotniece, M.; Roze, M.; Kalnachs, J.; Shlihta, G.; Shipkovs, P.; Kampars, V.; Tokmakov, A. *Eur. Phys. J. Appl. Phys.* **2007**, *40*, 169–173.
(30) Hayakawa, A.; Yoshikawa, O.; Fujieda, T.; Uehara, K.; Yoshikawa, S. *Appl. Phys. Lett.* **2007**, *90*, 163517.
(31) Li, H.; Jensen, T. J.; Fronczek, F. R.; Vicente, M. G. H. *J. Med. Chem.* **2008**, *51*, 502–511.
(32) Barger, W. R.; Hur, E.; Ferraudi, G.; Leznoff, C. C.; Nyokong, T.; Rosenthal, I.; Snow, A. W.; Stillman, M. J.; Wöhrle, D. In *Phthalocyanines, Properties and Applications*; Leznoff, C. C., Lever, A. B. P., Eds.; VCH Publishers, Inc.: New York, 1989; Vol. 1.
(33) Erb, T.; Zhokhavets, U.; Gobsch, G.; Raleva, S.; Stühn, B.; Schilinsky, P.; Waldauf, C.; Brabec, C. J. *Adv. Funct. Mater.* **2005**, *15*, 1193–1196.
(34) Brown, P. J.; Thomas, D. S.; Köhler, A.; Wilson, J. S.; Kim, J.-S.; Ramsdale, C. M.; Sirringhaus, H.; Friend, R. H. *Phys. Rev. B* **2003**, *67*, 064203.
(35) Vogel, M.; Doka, S.; Breyer, Ch.; Lux-Steiner, M. Ch.; Fostiropoulos, K. *Appl. Phys. Lett.* **2006**, *89*, 163501.
(36) Glatthaar, M.; Riede, M.; Keegan, N.; Sylvester-Hvid, K.; Zimmermann, B.; Niggemann, M.; Hinsch, A.; Gombert, A. *Sol. Energy Mater. Sol. Cells* **2007**, *91*, 390–393.
(37) Li, G.; Yao, Y.; Yang, H.; Shrotriya, V.; Yang, G.; Yang, Y. *Adv. Funct. Mater.* **2007**, *17*, 1636–1644.
(38) The HOMO and LUMO levels are taken from several references: $HOMO_{SiPc} = 5.3$ eV, $LUMO_{SiPc} = 3.4$ eV (ref 39), $HOMO_{P3HT} = 4.7$ eV (ref 40), and $LUMO_{PCBM} = 3.7$ eV (ref 41).
(39) Cheng, G.; Peng, X.; Hao, G.; Kennedy, V. O.; Ivanov, I. N.; Knappenberger, K.; Hill, T. J.; Rodgers, M. A. J.; Kenney, M. E. *J. Phys. Chem. A* **2003**, *107*, 3503–3514.
(40) Onoda, M.; Tada, K.; Nakayama, H. *J. Appl. Phys.* **1999**, *86*, 2110–2115.
(41) Brabec, C. J.; Cravino, A.; Meissner, D.; Sariciftci, N. S.; Fromherz, T.; Rispens, M. T.; Sanchez, L.; Hummelen, J. C. *Adv. Funct. Mater.* **2001**, *11*, 374–380.
(42) Yang, X.; Loos, J.; Veenstra, S. C.; Verhees, W. J. H.; Wienk, M. M.; Kroon, J. M.; Michels, M. A. J.; Janssen, R. A. J. *Nano Lett.* **2005**, *5*, 579–583.
(43) Kudo, N.; Honda, S.; Shimazaki, Y.; Ohkita, H.; Ito, S.; Benten, H. *Appl. Phys. Lett.* **2007**, *90*, 183513.
(44) Liu, Y.; Summers, M. A.; Edder, C.; Fréchet, J. M. J.; McGehee, M. D. *Adv. Mater.* **2005**, *17*, 2960–2964.
(45) Scully, S. R.; Armstrong, P. B.; Edder, C.; Fréchet, J. M. J.; McGehee, M. D. *Adv. Mater.* **2007**, *19*, 2961–2966.

AM800229P